

SCALABLE INFLUENCE AND FACT TRACING FOR LARGE LANGUAGE MODEL PRETRAINING

Anonymous authors

Paper under double-blind review

ABSTRACT

Training data attribution (TDA) methods aim to attribute model outputs back to specific training examples, and the application of these methods to large language model (LLM) outputs could significantly advance model transparency and data curation. However, it has been challenging to date to apply these methods to the full scale of LLM pretraining. In this paper, we introduce a gradient-based method that works effectively at scale, allowing us to retrieve influential examples for an 8B-parameter language model from a pretraining corpus of over 160B tokens with no need for subsampling or pre-filtering. Our method combines several techniques, including optimizer state correction, a task-specific Hessian approximation, and normalized encodings, which we find to be critical for performance at scale. Our method performs best at identifying examples that *influence* model predictions, but classical, model-agnostic retrieval methods such as BM25 still perform better at finding passages which explicitly contain relevant facts. These results demonstrate a misalignment between factual *attribution* and causal *influence*. With increasing model size and training tokens, we find that influence more closely aligns with attribution. Finally, we examine different types of examples identified as influential by our method, finding that while many directly entail a particular fact, others support the same output by reinforcing priors on relation types, common entities, and names.

1 INTRODUCTION

Modern large language models (LLMs) perform extraordinarily well at a wide variety of natural language tasks, but exactly how they leverage training data to achieve such capabilities is not well understood. One promising avenue of research to study this is *training data attribution* (TDA), which aims to identify influential training examples for given model predictions. When successful, TDA can serve as a method to both inspect and intervene on the training process. For example, it can enable training data curation targeted at specific tasks (Engstrom et al., 2024), reduction of data contamination (Mozes et al., 2023), and better transparency into model predictions (Grosse et al., 2023; Choe et al., 2024).

However, the steep computational cost of applying TDA approaches to LLMs has limited work in this area. Studies applying TDA to LLM fine-tuning have achieved promising results identifying examples that influence model behavior (Akyurek et al., 2022; Xia et al., 2024; Park et al., 2023), but there is significant evidence that much of an LLM’s knowledge and capabilities originates from pretraining (Hoffmann et al., 2022; Chang et al., 2024). Previous work applying TDA to pretraining has either focused on small models (Engstrom et al., 2024) or extremely few target queries, e.g. retrieving influential examples from a significantly subsampled corpus for less than 30 model predictions (Grosse et al., 2023; Choe et al., 2024). In our work, we scale TDA experiments to LLMs up to 8B parameters, thousands of model predictions, and corpora up to 160B tokens.

Specifically we propose TrackStar, a gradient-based influence method that combines innovations from previous work and scales to large setups (§3), while still supporting efficient retrieval of influential examples and quantitative evaluation. At scale, our method significantly outperforms previous influence methods at retrieving pretraining examples that entail a fact (*attribution*) and examples that influence specific factual predictions (*influence*) (§5, §6). Importantly, we demonstrate a misalignment between attribution and influence; classical methods such as BM25 are better at retrieving

054
055
056
057
058
059
060
061
062
063
064
065
066
067
068
069
070
071
072
073
074
075
076
077
078
079
080
081
082
083
084
085
086
087
088
089
090
091
092
093
094
095
096
097
098
099
100
101
102
103
104
105
106
107

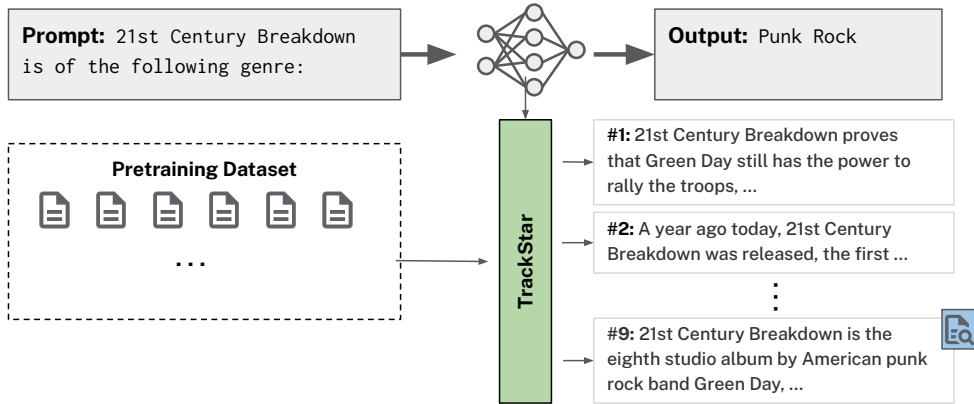


Figure 1: Top proponents from C4 using TrackStar given a factual query and model prediction. TrackStar is a gradient-based method that approximates *influence* on the model, which we show may not always be optimal for *attribution*, which involves finding examples which directly entail the target factual prediction.

examples that entail factual predictions, but those examples are not necessarily those that most affect model predictions (§5.1). We show that influence grows closer to attribution as models scale, both in parameters and training tokens (§5.3). To provide insights into where attribution and influence misalign, we include analyses of examples that have high influence for factual predictions in LLMs (§7). For example, rather than containing a full statement of a fact of interest, many examples appear to support priors on relation types, common entities, or names.

2 BACKGROUND: TRAINING DATA ATTRIBUTION

Researchers have proposed a variety of methods to measure the influence of individual training examples on output model metrics (e.g. loss on target datasets). Some of the best results come from simulation-based methods such as Datamodels (Ilyas et al., 2022) and Simfluence (Guu et al., 2023), which estimate contributions based on multiple training runs with different data subsets. However, this is not tractable for LLM pretraining, which is expensive to perform even once. For computational tractability, we focus on *gradient-based methods* that use parametric approximations, based on a single model, to predict how a model’s behavior would change under the removal (or addition) of specific training examples.

To quantify the influence from a training example z_m to an evaluation (query) example z_q , most gradient-based influence methods compute some version of a Hessian-corrected dot product $-\nabla L(z_q)H^{-1}\nabla L(z_m)$ of model gradients for z_m and z_q loss (Koh & Liang, 2017; Schioppa et al., 2022; Park et al., 2023; Grosse et al., 2023). Here, H^{-1} is the inverse Hessian matrix of the loss with respect to model parameters. The resulting dot product approximates changes in z_q loss from adding example z_m during training. In practice, existing methods use a variety of methods to approximate the Hessian H , notably the autocorrelation matrix $\tilde{\Phi}^T\tilde{\Phi} \in \mathbb{R}^{|\theta| \times |\theta|}$ of per-example gradients in TRAK (Park et al., 2023; Sagun et al., 2018) or the closely-related approximate curvature matrix G of EK-FAC (Grosse et al., 2023). These methods also tie closely back to TracIn (Pruthi et al., 2020), which computes gradient dot products aggregated over model checkpoints; recent work using TracIn has included gradient second moment correction (Akyurek et al., 2022; Xia et al., 2024), equivalent to a diagonal Hessian approximation (§3).

However, when applying influence methods to LLM pretraining, an additional bottleneck is the scale of model parameters and pretraining data. Given $|\theta|$ model parameters (on the order of billions), we have loss gradients $\nabla L(z) \in \mathbb{R}^{|\theta|}$ and inverse Hessian $H^{-1} \in \mathbb{R}^{|\theta| \times |\theta|}$. To rank pretraining examples, the gradient dot product must be computed between every pretraining example z_m (on the order of millions to billions) and the target query z_q . For this reason, previous work has focused on identifying influential examples during fine-tuning (Akyurek et al., 2022; Park et al., 2023; Xia et al., 2024) or during pretraining for smaller models (Engstrom et al., 2024). Closest to our work has been that of Grosse et al. (2023) and Choe et al. (2024) which looks at billion-parameter LLMs;

108 however, these perform retrieval on a small subset of the pretraining corpus and report only qualita-
109 tive evaluation on a small number of queries.

111 3 METHOD: TRACKSTAR

112 Here, we introduce TrackStar, a gradient-based influence method that combines innovations from
113 previous work that scales effectively to large settings. Following the gradient-based methods in
114 §2, we compute the influence between two examples as the dot product between the projected and
115 corrected model gradients for those examples. Because correction terms vary substantially in previ-
116 ous work, here we describe the motivation behind our specific approach, with ablation experiments
117 in §5.2. Specifically, given a query z_q (an input prompt with corresponding model completion or
118 desired completion) and a training example z_m , we compute the influence from z_m to z_q as:

$$119 \mathcal{I}_\theta(z_m, z_q) = \bar{G}_\theta(z_m) \cdot \bar{G}_\theta(z_q) \quad (1)$$

120 where $\bar{G}_\theta(z)$ is the projected, Hessian-corrected, and unit normalized gradient for example z given
121 model parameters θ :

$$122 \bar{G}_\theta(z) = \frac{G_\theta(z)}{\|G_\theta(z)\|_2} \quad G_\theta(z) = R^{-\frac{1}{2}} P_d \frac{\nabla_\theta \text{Loss}(z, \theta)}{\sqrt{V}} \quad (2)$$

123 In turn, we define:

- 124 • **Loss gradient** : $\nabla_\theta \text{Loss}(z, \theta) \in \mathbb{R}^{|\theta|}$: As in previous work, we compute the loss gradient for
125 each example z with respect to model parameters θ (Pruthi et al., 2020; Akyurek et al., 2022;
126 Han & Tsvetkov, 2022; Grosse et al., 2023; Xia et al., 2024). The original TRAK method uses
127 the multi-class margin function gradient; we evaluate different output functions in §A.2.1, but
128 we find that loss gradients perform best empirically. For each example z , we sum gradients
129 over target tokens; for training examples, this comprises all tokens in the example. If an input
130 prompt is given, we only include tokens in the model completion. In contrast to previous work
131 that selects only a subset of layers (Akyurek et al., 2022; Yeh et al., 2022; Grosse et al., 2023),
132 we compute gradients with respect to all model parameters θ except the token embedding layer,
133 pooled into layer blocks (§A.2.2) before dimensionality reduction with random projection.
- 134 • **Second moment estimate** : $V \in \mathbb{R}^{|\theta|}$: To account for high-magnitude gradient components
135 that might dominate gradient dot products (e.g. for outlier model components; Timkey & van
136 Schijndel, 2021; Puccetti et al., 2022), we correct by an estimate of the expected magnitude of
137 the loss gradient with respect to each model parameter. Formally, for each parameter $x \in \theta$,
138 this is an estimate of the second moment $\mathbb{E}_z((\nabla_x \text{Loss}(z, \theta))^2)$ of the gradient with respect to x .
139 These estimates are used by common optimizers such as Adafactor (Shazeer & Stern, 2018) and
140 Adam (Kingma & Ba, 2015), and as such the gradients corrected by V can be seen also as more
141 faithful to the model’s training process (Pruthi et al., 2020). We use the estimates of V computed
142 by Adafactor, which can be efficiently applied by element-wise multiplication.
143 Notably, dividing by the square root second moment \sqrt{V} is equivalent to using only the di-
144 agonal of the Gauss-Newton Hessian approximation (gradient autocorrelation matrix R around
145 zero; Sagun et al., 2018) from previous work (§2). Unlike TRAK (Park et al., 2023; Engstrom
146 et al., 2024), which corrects gradients by the autocorrelation after random projection, the opti-
147 mizer second moment estimates allow us to apply the correction per parameter before random
148 projection, enabling more granular correction of individual outlier components.
- 149 • **Random projection** : $P_d \in \mathbb{R}^{d \times |\theta|}$: As in TRAK (Park et al., 2023; Engstrom et al., 2024) and
150 as described in the original TracIn paper (Pruthi et al., 2020), we use Gaussian random projection
151 to reduce the dimensionality of the full model gradients. To improve projection efficiency, we use
152 the two-sided projection from Pruthi et al. (2020), which is equivalent to the recently proposed
153 LoGra method of dimensionality reduction (Choe et al., 2024; §A.2.2). This approach contrasts
154 with Grosse et al. (2023), who use either un-projected model gradients or query-specific low-rank
155 reductions. Un-projected model gradients are too large to store for all pretraining examples, and
156 query-specific approximations require that all pretraining example gradients be re-computed if a
157 new query is considered. Random projections allow the projected gradient to be computed and
158 saved exactly once per pretraining example, usable for all future retrievals. We use projection
159 dimensionality $d = 2^{16}$, but we experiment with lower dimensionalities in §5.2.

- **Hessian approximation** : $R^{-\frac{1}{2}} \in \mathbb{R}^{d \times d}$: With optimizer second moment estimates alone, we still find that retrievals suffer from common proponents that largely mimic the task template. To improve this, we follow Park et al. (2023) and Engstrom et al. (2024) in using the autocorrelation matrix $R = \tilde{\Phi}^T \tilde{\Phi}$ of per-example gradients as a Gauss-Newton approximation to the loss Hessian. We compute and apply this after optimizer state correction and random projection. For efficiency, we enforce a block-diagonal structure (§A.2.3) which allows us to efficiently compute $R^{-\frac{1}{2}}$ (Eq. 2). Departing from previous work, we consider a mixing approach where the matrix R_{train} estimated from the pretraining dataset is mixed with R_{eval} derived from the evaluation set:

$$R = \lambda R_{\text{eval}} + (1 - \lambda) R_{\text{train}} \quad (3)$$

This mixture allows $R^{-\frac{1}{2}}$ to downweight high-magnitude components that are common for evaluation examples in a task, such as components corresponding to the task template. We select the mixing parameter λ such that the top ~ 1000 task-specific gradient components (out of 65K) are downweighted (details in §A.2.3). For T-REx closed set experiments (§5), we use $\lambda = 0.90$; for C4 open set experiments (§6), we use $\lambda = 0.99$.¹

- **Unit normalization**: To compute cosine similarity, we unit normalize both input vectors in Equation 1, as in Akyurek et al. (2022), Han & Tsvetkov (2022), Choe et al. (2024), and Xia et al. (2024). This reduces the effect of outlier training examples that have high overall gradient magnitudes (Barshan et al., 2020; Han & Tsvetkov, 2021) and thus appear as common proponents before unit normalization. Unit norming is equivalent to ℓ -relative influence (Barshan et al., 2020), which is theoretically motivated to identify training examples that maximize the query example loss change while constraining the overall loss change.

Using the dot product of unit normed vectors $\bar{G}_\theta(z)$ (Equation 2) to quantify the influence $\mathcal{I}_\theta(z_m, z_q)$ of each training example z_m on query z_q , we are able to retrieve the top k training examples for z_q . We refer to these top-ranking examples as proponents of z_q (Pruthi et al., 2020). In the spirit of TracIn and TRAK, we refer to our proponent ranking method as Trac*, or “TrackStar”.

4 MODELS, DATASETS, AND METRICS

We apply TrackStar to identify proponent examples for factual predictions in LLMs up to 8B parameters. Unless otherwise specified, we first build an index of the projected gradients for all candidate examples of interest (e.g. the pretraining set), then compute the Hessian approximation R using a single pass over the data. For gradient-based methods, we perform exact scoring between each query and all candidate examples, with no need for lexical pre-filtering (c.f. Akyurek et al., 2022; Park et al., 2023; Grosse et al., 2023). All elements of this approach have compute cost linear in model and dataset size (§2).

4.1 MODELS

We pretrain a decoder-only language model on two epochs of English C4 (Raffel et al., 2020) for three model sizes: 154M, 1B, and 8B parameters, using the architecture described in Chowdhery et al. (2023) and implemented using T5X (Roberts et al., 2022). For all model sizes, we use a SentencePiece tokenizer (Kudo & Richardson, 2018) trained on C4 data with vocabulary size 32K. Using this tokenizer, English C4 consists of 160B tokens across 365M examples (short passages and documents). We pretrain with batch size 1024 and sequence length 2048 for two epochs (187K steps). All model sizes are trained on the same shuffle of the pretraining data. Exact hyperparameters are in Table A.4. The 154M, 1B, and 8B models reach eval losses (log-perplexities) of 2.34, 1.99, and 1.77 respectively. We focus primarily on the 8B model, but we study the smaller models for dimensionality ablations (§5.2) and scaling (§5.3).

4.2 FACT TRACING DATASET

We focus on identifying proponent examples for factual predictions in LLMs. For factual recall prompts, we use the filtered T-REx dataset from KILT (Petroni et al., 2021), which consists of entity-relation-entity triples such as (*Carleton College, country, USA*). We merge the KILT dataset back

¹Described in §A.2.3, C4 requires larger λ because the pretraining example gradients tend to be larger than those for T-REx sentences, due to longer sequence lengths.

216 into the original T-REx dataset (Elsahar et al., 2018), obtaining a dataset of facts with corresponding
 217 entity IDs, surface form aliases, and Wikipedia abstract sentences containing each fact.² For each
 218 fact, there are an average of 2.5 “ground-truth” entailing sentences out of 19.6M sentences total.
 219 After filtering out ambiguous prompts (e.g. multiple correct target entity IDs), we have a total of
 220 1.2M fact triples covering 97 relation types. Following Kandpal et al. (2023), we also annotate facts
 221 with the count (fact frequency) of pretraining examples from C4 that mention both entities.

222 We manually write natural language templates for all 97 relation types, so that a left-to-right LLM
 223 can predict the target fact as a completion, e.g. “*Carleton College is located in the following coun-*
 224 *try: USA*”. We mark predictions as correct using string matching after lowercasing and stopword
 225 removal, considering multiple possible correct surface form aliases as provided by KILT. Random
 226 chance accuracy on this task is close to 0% due to the large number of possible completions; our
 227 154M, 1B, and 8B models achieve 16.3%, 28.0%, and 32.4%, respectively. For factual queries
 228 in all following evaluations, we use a fixed sample of 5415 facts drawn randomly from this set
 229 but balanced for fact frequency and down-sampling for common target entities (such as “USA” or
 230 “English”), and limiting facts that are incorrectly predicted by all models. Each query contains
 231 an input prompt and ground truth target text. Dataset details and pre-processing are described in
 232 §A.3, and the exact set of 5415 evaluation queries is included in the supplementary material and at
 233 <http://to.be.released/camera/ready/>. Results for other templates are in §A.4.1

234 4.3 EVALUATION METRICS

235 After retrieving proponents for a given query, we consider traditional fact tracing metrics (MRR
 236 and recall, *attribution*; Akyurek et al., 2022) and a tail-patch metric that quantifies the effect of
 237 proponents on the model itself (*influence*).

238 **Attribution metrics: MRR and Recall@10.** These measure whether we retrieve examples that
 239 logically support (entail) a fact. For T-REx evaluations (§5), entailing Wikipedia abstract sentences
 240 are annotated in the dataset (§4.2). For C4 evaluations (§6), because passages are not annotated, we
 241 use an entailment model to score whether a candidate passage contains factual information support-
 242 ing the query. Specifically, we use a fine-tuned T5 11B (Raffel et al., 2020) model trained on ANLI
 243 (Nie et al., 2020) and synthetic data as described in Gekhman et al. (2023). Because C4 passages can
 244 be up to 2048 tokens, we split the input C4 passages by sentences using regex matching, and we take
 245 the maximum entailment score using a sliding window of three sentences as the input premise and
 246 the factual query as the hypothesis. We mark a proponent as entailing when this entailment score
 247 ≥ 0.50 .³ For MRR, we compute the mean reciprocal rank of the top-ranked “entailing” proponent
 248 for each fact. For recall@10, we compute the proportion of facts for which an entailing proponent
 249 appears in the top 10 proponent retrievals.

250 **Influence metric: incremental training probability increase (tail-patch).** Both of the previous
 251 metrics assume that the top-ranked proponents should be those that *entail* the target fact. However,
 252 these proponents are not necessarily the examples that would most influence the model to make
 253 that prediction. Following Koh & Liang (2017), most work on influence methods derives metrics
 254 from leave-one-out or other ablate-and-retrain experiments such as linear datamodeling score (Ilyas
 255 et al., 2022). However, this is not tractable for full-scale LLM pretraining, so we instead estimate
 256 the *additive* contribution from incremental training. Starting from the final model checkpoint and
 257 maintaining all pretraining hyperparameters, we take a single training step—which we call a *tail-*
 258 *patch* step—on a single retrieved proponent and measure the change in probability of the target
 259 sequence. We then average this change across the top $k = 10$ proponents for each query, and across
 260 all queries in the evaluation set. Results for different k are reported in §A.4.2.

261 4.4 BASELINE METHODS

262 We compare four ranking methods to retrieve proponent examples: **BM25** (Kamphuis et al., 2020),
 263 **Gecko** embeddings (Lee et al., 2024), **TRAK** (Park et al., 2023; Engstrom et al., 2024), and our

264 ²Because T-REx is automatically scraped, there is some inherent noise in the “ground truth” labels.

265 ³Based on blinded manual annotation of 100 C4 passages marked as entailing and non-entailing respectively,
 266 we find a false positive rate of 13% and a false negative rate of 11%. Of the incorrect annotations, most (54%)
 267 are fuzzy entailments where a passage implies but technically may not entail a fact.

method, **TrackStar**. As described in §5.2, we also implicitly compare to methods from several previous studies by ablating different correction terms from TrackStar. As a classical retrieval baseline, BM25 is a bag-of-words method that ranks candidates according to query terms appearing in each document, with TF-IDF weighting (“Lucene accurate” version; Kamphuis et al., 2020). Gecko is a text embedding model trained with a two-step distillation procedure and contrastive loss (Lee et al., 2024).⁴ TRAK is a gradient-based influence method that has been shown to perform well in previous work; the recommended version of TRAK in Park et al. (2023) and Engstrom et al. (2024) is similar to TrackStar but uses the multi-class margin gradient and a non-task-specific Hessian approximation, with no optimizer second moment correction or unit norm.⁵

5 T-REX CLOSED SET EVALUATION

We first evaluate TrackStar at fact tracing and influence on the T-REx dataset (§5.1), and we find that it outperforms prior gradient-based TDA methods (§5.2). For each query we retrieve the top 10 highest scoring candidate sentences from the set of 19.6M Wikipedia abstract sentences in T-REx.

5.1 T-REX CLOSED SET RESULTS

In Table 1, our results show that TrackStar outperforms other variants at identifying proponent examples for both attribution (identifying fact-entailing proponents) and influence (tail-patching scores) in the 8B model. Notably, previous work (Akyurek et al., 2022; Park et al., 2023) on this task considered only small candidate sets of 300 “distractors” per query, but we retrieve from the entire set of 19.6M sentences. We observe that this makes a significant difference in performance: while our TRAK replication achieves an MRR of 0.401 when replicating the smaller setting (similar to as reported by Park et al., 2023), it only achieves an MRR of 0.001 (and *negative* tail patch scores) in the full setting evaluated here. We find that this poor performance is largely due to the use of multi-class margin function gradients with correction applied per example rather than per token (§A.2.1), along with the lack of unit normalization (Table 1, Experiment 1 vs. Experiment 2). This result highlights that methods that perform well in small settings and classification tasks may be susceptible to noise in larger settings with LLMs.

We also find that classical, model-agnostic retrieval approaches (BM25 and Gecko) are significantly better than gradient-based influence methods at attribution (i.e. retrieving proponents that entail a given fact; MRR and recall; Table 1). Despite this, proponents from these classical methods still have *much less influence* on model predictions than proponents from influence methods. Tail-patching on proponents from BM25 (tail-patch score +0.41%) increase target fact probabilities by $2.2\times$ less than proponents from TrackStar (tail-patch score +0.90%). Even tail-patching on “ground truth” entailing sentences from T-REx (tail-patch score +0.52%) results in much smaller probability changes than proponents from TrackStar.⁶ This result suggests a distinction between *attribution* and *influence*; while classical, model-agnostic retrieval methods perform well at attribution (which we note is highly lexical and well-suited for string matching methods such as BM25; Wang et al., 2021), influence methods better predict how a proponent might affect the model and may better reflect the model’s reasoning (§7).

5.2 ABLATION EXPERIMENTS

Correction terms: In Table 1, we conduct ablations (labeled by experiment numbers) to determine the source of improvements for TrackStar over other gradient-based influence methods. Many of these ablations are close or equivalent to methods from previous work. For example, Experiment 1 corresponds closely to Pruthi et al. (2020), without the use of multiple checkpoints, while Experi-

⁴We use the $d = 768$ embedding model `textembedding-gecko@003` available on Google Cloud.

⁵TRAK has one additional difference, in that it multiplies scores by $Q = 1 - \bar{p}$, where \bar{p} is the probability of the candidate sequence, averaged over tokens. We find Q ranges from 0.6 to 1.0 across candidate sequences, and it has little effect on MRR, recall, and tail-patch scores. Theoretical motivations are described in §A.2.1.

⁶This echoes results from Park et al. (2023) for fact fine-tuning, but their results are based on TRAK retrievals from only 300 candidates, where one third of candidates are already the top BM25 retrievals. Based on our experiments, TRAK is prone to distractors in larger setups, resulting in poor tail-patch performance.

324
325
326
327
328
329
330
331
332
333
334
335
336
337
338
339
340
341
342
343
344
345
346
347
348
349
350
351
352
353
354
355
356
357
358
359
360
361
362
363
364
365
366
367
368
369
370
371
372
373
374
375
376
377

Exp. #	Optim.	R	Unit norm	MRR	Recall@10	Tail-patch
T-REx gold	–	–	–	Gold	Gold	+0.52%
BM25	–	–	–	0.592	0.773	+0.41%
Gecko	–	–	✓	0.620	0.794	+0.31%
TRAK		✓*		0.001	0.001	–0.02%
1				0.064	0.114	+0.35%
2			✓	0.266	0.358	+0.65%
3		✓	✓	0.290	0.399	+0.85%
4	✓		✓	0.300	0.413	+0.71%
5	✓	✓	✓	0.295	0.406	+0.87%
TrackStar	✓	Mixed	✓	0.365	0.496	+0.90%

Table 1: Results on T-REx closed set evaluation for the 8B-model (§5). Our setup is significantly more difficult than prior work, retrieving from all 20M T-REx abstract sentences rather than 300 “distractors” per fact. Classical retrieval results are reported in the top section for comparison. We note TRAK uses multi-class margin function gradients rather than loss gradients; details in §A.2.1.

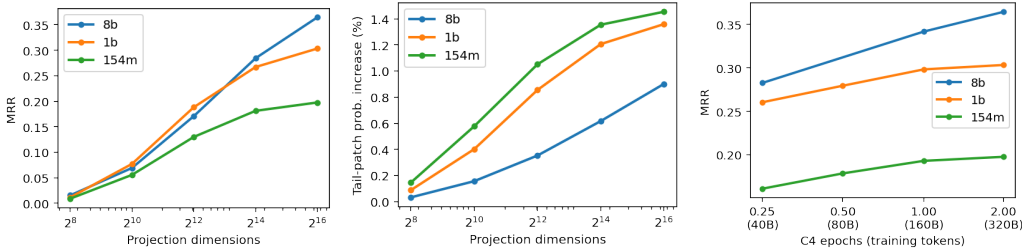


Figure 2: Left, center: attribution (MRR) and influence (tail-patch) scores as a function of gradient projection dimensionality d for different model sizes (§5.2). Right: attribution (MRR) scores throughout pretraining for different model sizes. As models improve, TrackStar influence becomes more similar to attribution (higher MRR; §5.3).

ment 2 corresponds to Han & Tsvetkov (2022) and Han et al. (2023). Experiment 3 is the method of Choe et al. (2024), and Experiment 4 corresponds to Akyurek et al. (2022) and Xia et al. (2024).⁷

First, we find that unit normalization is key to good MRR, recall, and tail-patch scores (Experiments 1–2; also verified by ablating unit normalization from other experiments). Optimizer second moment correction provides additional improvement, similar to including the Hessian approximation R (Experiments 3–4); intuitively, both methods perform Hessian correction by approximating the Hessian with gradient variance terms (§3). Using both optimizer state correction and R produces marginally better tail-patch scores but marginally worse MRR and recall (Experiment 5), compared to optimizer correction alone. Finally, the mixed task-specific Hessian approximation R (downweighting common gradient components for the fact completion task; §3) provides substantial improvements, particularly for MRR and recall.

In fact, on a theoretical basis, it may be somewhat surprising that unit normalization and task-specific Hessian approximation improve tail-patch scores at all. These two normalizations encourage the scoring method to focus on proponents specific to the target fact by downweighting proponents that affect loss overall (or loss for the overall task). These downweighted proponents might still be expected to have high tail-patch scores (large effects on target fact probability), despite their significant effect on loss overall, because tail-patch scores do not constrain the overall loss change induced by a proponent. The fact that these downweighted proponents actually have lower tail-patch scores (i.e. lower tail-patch scores for proponents before unit normalization and task-specific Hessian correction) indicates that these corrections actually have an overall denoising effect. Despite their motivation based on maximizing target influence under overall loss change constraints, these corrections actually find proponents that maximize target influence even without such constraints.

Projection dimensionality: Higher gradient projection dimensionality d results in higher fidelity representations, but both the memory required to store projected gradients and the retrieval cost to compute dot products increase (linearly) with d . To balance these considerations, in Figure 2 (left,

⁷Xia et al. (2024) also normalize by Adam first moment estimates, but these are not available in Adafactor.

Method	MRR	Recall@10	Tail-patch
BM25	0.687	0.845	+0.83%
Gecko	0.636	0.826	+0.54%
GRADIENT DOT PRODUCT	0.003	0.015	+0.04%
GRADIENT COSINE	0.252	0.393	+1.95%
TrackStar	0.338	0.515	+2.11%

Table 2: Results retrieving proponents from all of C4 (§6). GRADIENT COSINE ablates the Hessian approximation R from TrackStar, and GRADIENT DOT PRODUCT further ablates unit normalization.

center), we plot how attribution (MRR) and influence (tail-patch) scores improve with projection dimensionality for TrackStar.⁸ For smaller models (154M and 1B parameters), scores have begun to plateau around $d = 2^{16}$. Although the 8B-parameter model has not yet plateaued, we restrict our experiments to $d = 2^{16}$ due to memory limitations, as the index of 365M C4 examples at $d = 2^{16}$ is already 87TB in size (§6). Furthermore, we note that our factual knowledge task likely requires a large number of dimensions due to the inherent difficulty of compressing individual facts about a large number of entities; attribution and influence for other tasks might require far fewer dimensions.

5.3 INFLUENCE APPROACHES ATTRIBUTION

In §5.1, we demonstrated a distinction between *attribution* (identifying proponents that entail a fact, quantified by MRR and recall) and *influence* (identifying proponents that influence the model prediction, quantified by tail-patch scores). Interestingly, we find that TrackStar attribution scores improve as models increase in both parameters and training tokens (Figure 2, right). This indicates that as models improve, the influential examples that TrackStar identifies align more with attribution, suggesting that more capable models rely more on examples that actually entail facts for factual predictions. Of course, it does not appear that these constructs converge entirely; recall from §5.1 that tail-patching on ground truth entailing proponents results in much smaller target probability changes than TrackStar proponents, even for our largest model. Thus, it appears that as models improve, they are more likely to use actual entailing examples to learn facts, but there is still a large number of proponents that have large effects on the model despite non-entailment. A deeper analysis of these types of proponents is performed in §7.

6 C4 OPEN SET EVALUATION

While the T-REx setting is useful for controlled experiments, in practical use LLMs are trained from large, unsupervised corpora containing a wide variety of passages that the model may learn from. To extend TDA to this setting, we apply TrackStar to identify influential examples for our 8B-parameter model from all 365M passages in the C4 corpus. In this scenario, our candidate set (C4) consists of all training examples that the LLM has ever seen. These candidate sequences are often much longer than T-REx sentences (up to 2048 tokens), and they cover many domains rather than just Wikipedia.

For the same set of 5.4K factual queries with ground truth targets as §5, we retrieve proponents using TrackStar, BM25, and Gecko. As C4 is a much larger corpus and is proportionally more expensive to compute gradients over, we perform a more limited set of ablations as shown in Table 2. We focus on the two corrections that had the largest effects in §5.2: mixed task-specific Hessian approximation R (ablated in GRADIENT COSINE in Table 2) and unit normalization (further ablated in GRADIENT DOT PRODUCT in Table 2).⁹ Both of these ablated methods still significantly outperform original TRAK in §5. As before, we quantify performance using MRR, recall, and tail-patch scores.

6.1 C4 OPEN SET RESULTS

In line with §5.1, TrackStar has better tail-patch (*influence*) scores than all other methods, and better MRR and recall (*attribution*) than other gradient methods (Table 2). Again, we find that unit

⁸Park et al. (2023) find that performance may decrease if projection dimensionality is too large, though our experiments do not appear to be close to that limit.

⁹GRADIENT COSINE is equivalent to Experiment 4 in Table 1, and GRADIENT DOT PRODUCT is equivalent to Experiment 1 with optimizer second moment correction.

432
433
434
435
436
437
438
439
440
441
442
443
444
445
446
447
448
449
450
451
452
453
454
455
456
457
458
459
460
461
462
463
464
465
466
467
468
469
470
471
472
473
474
475
476
477
478
479
480
481
482
483
484
485

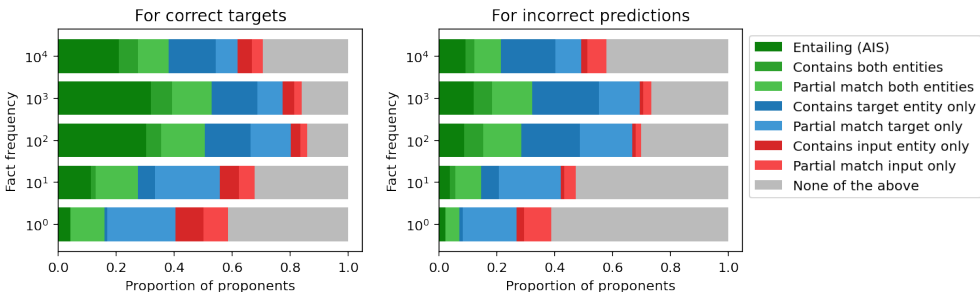


Figure 3: Proportions of TrackStar proponents (top 10 per query) retrieved from C4 that entail a prediction, contain both entities, or contain only one entity for a model prediction.

normalization (cosine) is critical to performance, and the addition of task-specific Hessian approximation R in TrackStar further improves results. In particular, lack of unit normalization often leads to retrieval of long irrelevant examples, as these tend to have large gradient magnitudes.

Also in line with §5, BM25 and Gecko perform much better than TrackStar for attribution (MRR 0.687 and 0.636 vs. 0.338). Still, we note overall high MRR and recall scores given the difficulty of the task: for 51.5% of facts, TrackStar retrieves an entailing example in the top 10 out of 365M C4 examples. Additionally, TrackStar performs over $2.5\times$ better than BM25 and Gecko at retrieving examples that influence model predictions (tail-patch score +2.11% vs. +0.83% and +0.54%). This reinforces the distinction between attribution and influence: examples that entail facts—such as proponents retrieved by BM25—are often not the examples that most affect a model’s predictions.

7 HEADROOM ANALYSIS

In §5 and §6 we showed that TrackStar makes significant progress towards attribution for LLM pretraining, outperforming other methods at retrieving *influential* pretraining examples, but it still falls short of classical baselines on the fact tracing task (*attribution*). To better understand why, we look in more detail at the types of proponents retrieved by our method. We find that much of the headroom can be explained by proponents which reflect priors or partial matches, multi-hop reasoning, or idiosyncrasies of the fact tracing task such as ambiguous entities or alternative correct answers. Examples of these proponents are included in Table A.1 and Table A.2.

Priors and partial matches: In an ideal world, model predictions would be informed by examples that fully describe (entail) that fact, and these would appear as the top proponents. However, the model’s output can also be informed by priors, such as the probability that the answer to any question about language being “*English*” or a city being “*New York*”. In Figure 3 (left), we examine the distribution of proponents (top 10 per query) from TrackStar based on their relation to the query: (1) a full entailment (as in §6), (2) containing the input and target entity but without entailing the fact, (3) containing only one of the entities, or (4) containing neither entity. The latter three categories are estimated by string-matching, and we also consider partial-matches where the proponent matches at least one non-stopword of an entity (e.g. a last name). Additionally, we stratify these categories by how frequently the fact appears in the pretraining corpus.

We find that a majority of proponents fall into one of the full- or partial-match categories, with close to 40% of proponents entailing the query on moderate-frequency (10^2 to 10^3 occurrences in C4) facts and 40% more with at least a partial match to one of the entities. While it is not clear why partial matches sometimes score more highly than entailing examples, it is plausible that especially when the target entity is mentioned, these examples would contribute to the model’s prior $P(y)$ of generating the target string; 62% of proponents contain at least a partial match to the target entity. For less common entities (e.g. less frequent facts), partial matches appear more frequently, such as matching the first name in “*Alemayehu Shumye*” in Table A.1. These may represent fallback reasoning, where the model does not know about the specific entity but makes a guess based on statistical associations, such as between names and nationalities.

486 Interestingly, we observe a drop in entailing and entity-matching proponents for the highest fre-
 487 quency facts ($\geq 10^4$ occurrences). In part, this appears due to data artifacts, as some examples in
 488 T-REx are string matches for common nouns, such as “*City is located in the following country:*
 489 *United States*”, and it is unclear how a model *should* interpret these queries. Additionally, there
 490 may be saturation effects (Pruthi et al., 2020), where these common facts (such as that Munich is a
 491 city in Germany in the “*Munich Symphony Orchestra*” example in Table A.1) are learned early in
 492 training, and gradients at the final checkpoint are diminished.

493 **Multi-hop reasoning:** We also observe some cases where there is a multi-step reasoning path be-
 494 tween a proponent text and the query. For example in the “*Carel Steven Adama van Sheltema*”
 495 example in Table A.1, a prompt asks about a person’s native language, and the first proponent pas-
 496 sage states that they were born in Amsterdam. While not strictly entailing, this does provide support
 497 for the model to plausibly guess that the language is “*Dutch*”.

498 **Noisy proponents:** However, some retrieved proponents are simply noisy. In a relatively small
 499 number of cases, examples are entirely irrelevant (e.g. “*Cadillac*” in Table A.1). In these cases, we
 500 often find that TrackStar and other gradient-based methods retrieve long or repetitive passages which
 501 bear minimal relation to the query, or which repeat the target string many times (e.g. “*Présent*”
 502 example in Table A.1; this may also reflect priors as discussed above). We suspect that this may be
 503 because training examples have gradients aggregated across an entire passage. Repeating statements
 504 that are tangentially relevant can add up to a substantial similarity score, and if better examples
 505 receive lower scores due to saturation or other effects, these distractors may rank as top proponents.
 506

507 7.1 DEBUGGING INCORRECT PREDICTIONS

508 Above, we examined proponent retrievals only for ground truth targets, even when the actual model
 509 prediction would have been incorrect. In a model-debugging scenario, however, it may be useful to
 510 attribute the *incorrect* predictions of the model so as to understand where this behavior was learned
 511 (Grosse et al., 2023; Nguyen et al., 2024) and uncover mislabeled examples or other issues with the
 512 training corpus. In Figure 3 (right) we consider the subset of 1592 queries from our evaluation set
 513 that the 8B model gets wrong, we retrieve proponents from C4 using TrackStar for the (incorrect)
 514 model prediction, and we categorize the proponents using the same scheme as §7.
 515

516 We observe that a substantial fraction (28.5%) of these answers actually do have entailing passages
 517 (7.1% of all proponents in Figure 3 right), and on closer inspection, we find that many of these
 518 correspond to alternative correct answers. For example, for “*Ricky Gervais works as: comedian*”
 519 the model predicts “*actor*” (he is both), and for “*Victoria Park is located in the following country:*
 520 *Australia*” the model predicts “*United Kingdom*” (there is a Victoria Park in both). However, a
 521 much larger fraction of proponents consist of partial matches, suggesting that when the model is
 522 wrong, it is often making a guess based on partial information, e.g. using one of the reasoning
 523 strategies or priors described in §7.
 524

525 8 CONCLUSION

526 In this paper, we explore data attribution (*influence*) methods at the scale of C4 pretraining for an
 527 8B-parameter LLM, pushing the frontier of TDA capabilities closer to full pretraining attribution
 528 for modern LLMs. Our best method, TrackStar, outperforms previous gradient-based methods both
 529 at retrieving examples that entail a fact (*attribution*) as well as examples that influence model pre-
 530 dictions (*influence*). Despite this, we find that classical, model-agnostic retrieval methods such as
 531 BM25 still perform better on attribution metrics. While this may be partially due to the highly lexi-
 532 cal nature of the fact tracing task (Akyurek et al., 2022; Wang et al., 2021), it also demonstrates that
 533 attribution and influence may not always be fully aligned, both due to headroom in the method and
 534 the fact that different types of non-entailing examples can be influential on a model’s prediction. We
 535 do find, however, that influence and attribution are more closely aligned as models improve. This
 536 suggests that TDA results may even align further with human intuition for newer generations of
 537 LLMs, potentially enabling practical usage of this technique to debug model predictions and better
 538 understand the connection between training data and model behavior.
 539

REFERENCES

- 540
541
542 Ekin Akyurek, Tolga Bolukbasi, Frederick Liu, Binbin Xiong, Ian Tenney, Jacob Andreas, and
543 Kelvin Guu. Towards tracing knowledge in language models back to the training data. In
544 *Findings of the Association for Computational Linguistics: EMNLP 2022*, pp. 2429–2446, Abu
545 Dhabi, United Arab Emirates, December 2022. Association for Computational Linguistics. URL
546 <https://aclanthology.org/2022.findings-emnlp.180>.
- 547 Elnaz Barshan, Marc-Etienne Brunet, and Gintare Karolina Dziugaite. RelatIF: Identifying explana-
548 tory training samples via relative influence. In *Proceedings of the Twenty Third International
549 Conference on Artificial Intelligence and Statistics*, volume 108, pp. 1899–1909, 2020. URL
550 <https://proceedings.mlr.press/v108/barshan20a>.
- 551 Hoyeon Chang, Jinho Park, Seonghyeon Ye, Sohee Yang, Youngkyung Seo, Du-Seong Chang, and
552 Minjoon Seo. How do large language models acquire factual knowledge during pretraining?
553 *arXiv*, 2024. URL <https://arxiv.org/abs/2406.11813>.
- 554 Sang Keun Choe, Hwijeen Ahn, Juhan Bae, Kewen Zhao, Minsoo Kang, Youngseog Chung, Adithya
555 Pratapa, Willie Neiswanger, Emma Strubell, Teruko Mitamura, Jeff Schneider, Eduard Hovy,
556 Roger Grosse, and Eric Xing. What is your data worth to GPT? LLM-scale data valuation with
557 influence functions. *arXiv*, 2024. URL <https://arxiv.org/abs/2405.13954>.
- 558 Aakanksha Chowdhery, Sharan Narang, Jacob Devlin, Maarten Bosma, Gaurav Mishra, Adam
559 Roberts, Paul Barham, Hyung Won Chung, Charles Sutton, Sebastian Gehrmann, Parker Schuh,
560 Kensen Shi, Sasha Tsvyashchenko, Joshua Maynez, Abhishek Rao, Parker Barnes, Yi Tay, Noam
561 Shazeer, Vinodkumar Prabhakaran, Emily Reif, Nan Du, Ben Hutchinson, Reiner Pope, James
562 Bradbury, Jacob Austin, Michael Isard, Guy Gur-Ari, Pengcheng Yin, Toju Duke, Anselm Lev-
563 skaya, Sanjay Ghemawat, Sunipa Dev, Henryk Michalewski, Xavier Garcia, Vedant Misra, Kevin
564 Robinson, Liam Fedus, Denny Zhou, Daphne Ippolito, David Luan, Hyeontaek Lim, Barret
565 Zoph, Alexander Spiridonov, Ryan Sepassi, David Dohan, Shivani Agrawal, Mark Omernick, An-
566 drew M. Dai, Thanumalayan Sankaranarayanan Pillai, Marie Pellat, Aitor Lewkowycz, Erica Mor-
567 eira, Rewon Child, Oleksandr Polozov, Katherine Lee, Zongwei Zhou, Xuezhi Wang, Brennan
568 Saeta, Mark Diaz, Orhan Firat, Michele Catasta, Jason Wei, Kathy Meier-Hellstern, Douglas Eck,
569 Jeff Dean, Slav Petrov, and Noah Fiedel. PaLM: Scaling language modeling with pathways. *Journal of Machine Learning Research*, 2023. URL <https://arxiv.org/abs/2204.02311>.
- 570
571 Hady Elsahar, Pavlos Vougiouklis, Arslan Remaci, Christophe Gravier, Jonathon Hare, Frederique
572 Laforest, and Elena Simperl. T-REx: A large scale alignment of natural language with knowledge
573 base triples. In *Proceedings of the Eleventh International Conference on Language Resources and
574 Evaluation (LREC 2018)*, Miyazaki, Japan, May 2018. European Language Resources Associa-
575 tion (ELRA). URL <https://aclanthology.org/L18-1544>.
- 576 Logan Engstrom, Axel Feldmann, and Aleksander Madry. DsDm: Model-aware dataset selection
577 with datamodels. In *Proceedings of the 41st International Conference on Machine Learning*,
578 pp. 12491–12526. PMLR, 21–27 Jul 2024. URL [https://proceedings.mlr.press/
579 v235/engstrom24a.html](https://proceedings.mlr.press/v235/engstrom24a.html).
- 580 Zorik Gekhman, Jonathan Herzig, Roei Aharoni, Chen Elkind, and Idan Szepktor. TrueTeacher:
581 Learning factual consistency evaluation with large language models. In *Proceedings of the
582 2023 Conference on Empirical Methods in Natural Language Processing*, pp. 2053–2070,
583 Singapore, December 2023. Association for Computational Linguistics. URL [https://
584 aclanthology.org/2023.emnlp-main.127](https://aclanthology.org/2023.emnlp-main.127).
- 585
586 Roger Grosse, Juhan Bae, Cem Anil, Nelson Elhage, Alex Tamkin, Amirhossein Tajdini, Benoit
587 Steiner, Dustin Li, Esin Durmus, Ethan Perez, Evan Hubinger, Kamilė Lukošiušė, Karina
588 Nguyen, Nicholas Joseph, Sam McCandlish, Jared Kaplan, and Samuel R. Bowman. Study-
589 ing large language model generalization with influence functions. *arXiv*, 2023. URL [https://
590 arxiv.org/abs/2308.03296](https://arxiv.org/abs/2308.03296).
- 591
592 Kelvin Guu, Albert Webson, Ellie Pavlick, Lucas Dixon, Ian Tenney, and Tolga Bolukbasi. Simflu-
593 ence: Modeling the influence of individual training examples by simulating training runs. *arXiv*,
2023. URL <https://arxiv.org/abs/2303.08114>.

- 594 Xiaochuang Han and Yulia Tsvetkov. Influence tuning: Demoting spurious correlations via in-
595 stance attribution and instance-driven updates. In *Findings of the Association for Computational*
596 *Linguistics: EMNLP 2021*, pp. 4398–4409, Punta Cana, Dominican Republic, November 2021.
597 Association for Computational Linguistics. URL [https://aclanthology.org/2021.](https://aclanthology.org/2021.findings-emnlp.374)
598 [findings-emnlp.374](https://aclanthology.org/2021.findings-emnlp.374).
- 599
600 Xiaochuang Han and Yulia Tsvetkov. ORCA: Interpreting prompted language models via locating
601 supporting data evidence in the ocean of pretraining data. *arXiv*, 2022. URL [https://arxiv.](https://arxiv.org/abs/2205.12600)
602 [org/abs/2205.12600](https://arxiv.org/abs/2205.12600).
- 603
604 Xiaochuang Han, Daniel Simig, Todor Mihaylov, Yulia Tsvetkov, Asli Celikyilmaz, and Tianlu
605 Wang. Understanding in-context learning via supportive pretraining data. In *Proceedings of the*
606 *61st Annual Meeting of the Association for Computational Linguistics (Volume 1: Long Papers)*,
607 pp. 12660–12673, Toronto, Canada, July 2023. Association for Computational Linguistics. URL
608 <https://aclanthology.org/2023.acl-long.708>.
- 609
610 Jordan Hoffmann, Sebastian Borgeaud, Arthur Mensch, Elena Buchatskaya, Trevor Cai, Eliza
611 Rutherford, Diego de Las Casas, Lisa Anne Hendricks, Johannes Welbl, Aidan Clark, Tom Hen-
612 nigan, Eric Noland, Katie Millican, George van den Driessche, Bogdan Damoc, Aurelia Guy,
613 Simon Osindero, Karen Simonyan, Erich Elsen, Oriol Vinyals, Jack W. Rae, and Laurent Sifre.
614 Training compute-optimal large language models. In *Advances in Neural Information Processing*
Systems, 2022. URL <https://arxiv.org/abs/2203.15556>.
- 615
616 Andrew Ilyas, Sung Min Park, Logan Engstrom, Guillaume Leclerc, and Aleksander Madry. Data-
617 models: Predicting predictions from training data. *arXiv*, 2022. URL [https://arxiv.org/](https://arxiv.org/abs/2202.00622)
618 [abs/2202.00622](https://arxiv.org/abs/2202.00622).
- 619
620 Chris Kamphuis, Arjen P. de Vries, Leonid Boytsov, and Jimmy Lin. Which BM25 do you mean?
621 A large-scale reproducibility study of scoring variants. In *Advances in Information Retrieval:*
622 *42nd European Conference on IR Research, ECIR 2020, Lisbon, Portugal, April 14–17, 2020,*
623 *Proceedings, Part II*, pp. 28–34, Berlin, Heidelberg, 2020. Springer-Verlag. URL [https://](https://doi.org/10.1007/978-3-030-45442-5_4)
doi.org/10.1007/978-3-030-45442-5_4.
- 624
625 Nikhil Kandpal, Haikang Deng, Adam Roberts, Eric Wallace, and Colin Raffel. Large language
626 models struggle to learn long-tail knowledge. In *International Conference on Machine Learning*,
627 2023. URL <https://arxiv.org/abs/2211.08411>.
- 628
629 Diederik P. Kingma and Jimmy Ba. Adam: A method for stochastic optimization. In *International*
630 *Conference on Learning Representations*, 2015. URL [https://arxiv.org/abs/1412.](https://arxiv.org/abs/1412.6980)
631 [6980](https://arxiv.org/abs/1412.6980).
- 632
633 Pang Wei Koh and Percy Liang. Understanding black-box predictions via influence functions. In
634 *Proceedings of the 34th International Conference on Machine Learning*, pp. 1885–1894, 2017.
URL <https://arxiv.org/abs/1703.04730>.
- 635
636 Taku Kudo and John Richardson. SentencePiece: A simple and language independent sub-
637 word tokenizer and detokenizer for neural text processing. In *Proceedings of the 2018 Con-*
638 *ference on Empirical Methods in Natural Language Processing: System Demonstrations*, pp.
639 66–71, Brussels, Belgium, November 2018. Association for Computational Linguistics. URL
<https://aclanthology.org/D18-2012>.
- 640
641 Jinhyuk Lee, Zhuyun Dai, Xiaoqi Ren, Blair Chen, Daniel Cer, Jeremy R. Cole, Kai Hui, Michael
642 Boratko, Rajvi Kapadia, Wen Ding, Yi Luan, Sai Meher Karthik Duddu, Gustavo Hernández
643 Abrego, Weiqiang Shi, Nithi Gupta, Aditya Kusupati, Prateek Jain, Siddhartha R. Jonnalagadda,
644 Ming-Wei Chang, and Iftexhar Naim. Gecko: Versatile text embeddings distilled from large
645 language models. *arXiv*, 2024. URL <https://arxiv.org/abs/2403.20327>.
- 646
647 Maximilian Mozes, Tolga Bolukbasi, Ann Yuan, Frederick Liu, Nithum Thain, and Lucas Dixon.
Gradient-based automated iterative recovery for parameter-efficient tuning. *arXiv*, 2023. URL
<https://arxiv.org/abs/2302.06598>.

- 648 Elisa Nguyen, Johannes Bertram, Evgenii Kortukov, Jean Y Song, and Seong Joon Oh. Towards
649 user-focused research in training data attribution for human-centered explainable AI. *arXiv*, 2024.
650 URL <https://arxiv.org/abs/2409.16978>.
- 651 Yixin Nie, Adina Williams, Emily Dinan, Mohit Bansal, Jason Weston, and Douwe Kiela. Adversarial
652 NLI: A new benchmark for natural language understanding. In *Proceedings of the 58th Annual
653 Meeting of the Association for Computational Linguistics*, pp. 4885–4901, Online, July 2020.
654 Association for Computational Linguistics. URL [https://aclanthology.org/2020.
655 acl-main.441](https://aclanthology.org/2020.acl-main.441).
- 656 Sung Min Park, Kristian Georgiev, Andrew Ilyas, Guillaume Leclerc, and Aleksander Madry.
657 TRAK: Attributing model behavior at scale. In *Proceedings of the 40th International Con-
658 ference on Machine Learning*, volume 202 of *Proceedings of Machine Learning Research*,
659 pp. 27074–27113. PMLR, 23–29 Jul 2023. URL [https://proceedings.mlr.press/
660 v202/park23c.html](https://proceedings.mlr.press/v202/park23c.html).
- 661 Fabio Petroni, Tim Rocktäschel, Sebastian Riedel, Patrick Lewis, Anton Bakhtin, Yuxiang Wu,
662 and Alexander Miller. Language models as knowledge bases? In *Proceedings of the 2019
663 Conference on Empirical Methods in Natural Language Processing and the 9th International
664 Joint Conference on Natural Language Processing (EMNLP-IJCNLP)*, pp. 2463–2473, Hong
665 Kong, China, November 2019. Association for Computational Linguistics. URL [https:
666 //aclanthology.org/D19-1250](https://aclanthology.org/D19-1250).
- 667 Fabio Petroni, Aleksandra Piktus, Angela Fan, Patrick Lewis, Majid Yazdani, Nicola De Cao,
668 James Thorne, Yacine Jernite, Vladimir Karpukhin, Jean Maillard, Vassilis Plachouras, Tim
669 Rocktäschel, and Sebastian Riedel. KILT: A benchmark for knowledge intensive language tasks.
670 In *Proceedings of the 2021 Conference of the North American Chapter of the Association for
671 Computational Linguistics: Human Language Technologies*, pp. 2523–2544, Online, June 2021.
672 Association for Computational Linguistics. URL [https://aclanthology.org/2021.
673 naacl-main.200](https://aclanthology.org/2021.naacl-main.200).
- 674 Garima Pruthi, Frederick Liu, Mukund Sundararajan, and Satyen Kale. Estimating training data
675 influence by tracing gradient descent. In *Advances in Neural Information Processing Systems*,
676 2020. URL <https://arxiv.org/abs/2002.08484>.
- 677 Giovanni Puccetti, Anna Rogers, Aleksandr Drozd, and Felice Dell’Orletta. Outlier dimensions that
678 disrupt transformers are driven by frequency. In *Findings of the Association for Computational
679 Linguistics: EMNLP 2022*, pp. 1286–1304, Abu Dhabi, United Arab Emirates, December 2022.
680 Association for Computational Linguistics. URL [https://aclanthology.org/2022.
681 findings-emnlp.93](https://aclanthology.org/2022.findings-emnlp.93).
- 682 Colin Raffel, Noam Shazeer, Adam Roberts, Katherine Lee, Sharan Narang, Michael Matena, Yanqi
683 Zhou, Wei Li, and Peter J. Liu. Exploring the limits of transfer learning with a unified text-to-text
684 transformer. *Journal of Machine Learning Research*, 21(1), 2020. URL [https://arxiv.
685 org/abs/1910.10683](https://arxiv.org/abs/1910.10683).
- 686 Adam Roberts, Hyung Won Chung, Anselm Levskaya, Gaurav Mishra, James Bradbury, Daniel
687 Andor, Sharan Narang, Brian Lester, Colin Gaffney, Afroz Mohiuddin, Curtis Hawthorne, Aitor
688 Lewkowycz, Alex Salcianu, Marc van Zee, Jacob Austin, Sebastian Goodman, Livio Baldini
689 Soares, Haitang Hu, Sasha Tsvyashchenko, Aakanksha Chowdhery, Jasmijn Bastings, Jannis Bu-
690 lian, Xavier Garcia, Jianmo Ni, Andrew Chen, Kathleen Kenealy, Jonathan H. Clark, Stephan Lee,
691 Dan Garrette, James Lee-Thorp, Colin Raffel, Noam Shazeer, Marvin Ritter, Maarten Bosma,
692 Alexandre Passos, Jeremy Maitin-Shepard, Noah Fiedel, Mark Omernick, Brennan Saeta, Ryan
693 Sepassi, Alexander Spiridonov, Joshua Newlan, and Andrea Gesmundo. Scaling up models and
694 data with `t5x` and `seqio`. *arXiv*, 2022. URL <https://arxiv.org/abs/2203.17189>.
- 695 Levent Sagun, Utku Evci, V. Ugur Guney, Yann Dauphin, and Leon Bottou. Empirical analysis of
696 the hessian of over-parametrized neural networks. *arXiv*, 2018. URL [https://arxiv.org/
697 abs/1706.04454](https://arxiv.org/abs/1706.04454).
- 698 Andrea Schioppa, Polina Zablotskaia, David Vilar Torres, and Artem Sokolov. Scaling up influence
699 functions. In *AAAI-22, 2022*. URL <https://arxiv.org/abs/2112.03052>.
- 700
701

- 702 Noam Shazeer and Mitchell Stern. Adafactor: Adaptive learning rates with sublinear memory
703 cost. In *Proceedings of the 35th International Conference on Machine Learning*, volume 80
704 of *Proceedings of Machine Learning Research*, pp. 4596–4604. PMLR, 10–15 Jul 2018. URL
705 <https://proceedings.mlr.press/v80/shazeer18a.html>.
706
- 707 William Timkey and Marten van Schijndel. All bark and no bite: Rogue dimensions in transformer
708 language models obscure representational quality. In *Proceedings of the 2021 Conference on*
709 *Empirical Methods in Natural Language Processing*, pp. 4527–4546, Online and Punta Cana,
710 Dominican Republic, November 2021. Association for Computational Linguistics. URL <https://aclanthology.org/2021.emnlp-main.372>.
711
- 712 Shuai Wang, Shengyao Zhuang, and Guido Zuccon. BERT-based dense retrievers require interpola-
713 tion with BM25 for effective passage retrieval. In *Proceedings of the 2021 ACM SIGIR Interna-*
714 *tional Conference on Theory of Information Retrieval, ICTIR ’21*, pp. 317–324, New York, NY,
715 USA, 2021. Association for Computing Machinery. URL [https://doi.org/10.1145/](https://doi.org/10.1145/3471158.3472233)
716 [3471158.3472233](https://doi.org/10.1145/3471158.3472233).
- 717 Mengzhou Xia, Sadhika Malladi, Suchin Gururangan, Sanjeev Arora, and Danqi Chen. LESS:
718 Selecting influential data for targeted instruction tuning. In *International Conference on Machine*
719 *Learning (ICML)*, 2024. URL <https://arxiv.org/abs/2402.04333>.
720
- 721 Chih-Kuan Yeh, Ankur Taly, Mukund Sundararajan, Frederick Liu, and Pradeep Ravikumar. First
722 is better than last for language data influence. In *Advances in Neural Information Processing Sys-*
723 *tems*, volume 35, pp. 32285–32298, 2022. URL <https://arxiv.org/abs/2202.11844>.
724

725 A APPENDIX

726 A.1 QUALITATIVE EXAMPLES

727
728
729
730
731
732
733
734
735
736
737
738
739
740
741
742
743
744
745
746
747
748
749
750
751
752
753
754
755

756
757
758
759
760
761
762
763
764
765
766
767
768
769
770
771
772
773
774
775
776
777
778
779
780
781
782
783
784
785
786
787
788
789
790
791
792
793
794
795
796
797
798
799
800
801
802
803
804
805
806
807
808
809**Example proponents from TrackStar:****Présent is in the following language: → English (incorrect, groundtruth: French)****Proponent retrieval #3 (non-entailing):**

Sorry, this entry is only available in Deutsch, English and All Languages. Sorry, this entry is only available in Nederlands, Slovenina, Franais, Polski, English and All Languages. Sorry, this entry is only available in English and All Languages. Sorry, this entry is only available in English and All Languages. Sorry, this entry is only available in Polski, English and ...

Victoria Park is located in the following country: → United Kingdom**(incorrect*, groundtruth: Australia)****Proponent retrieval #1 (entailing):**

Victoria Park in the northern part of Londons East end is 86 hectares of meadows, trees and formal gardens set around two lakes. The Regents Canal runs along the south and west sides of the park and is pleasant to walk along especially on a summer day. The park was donated to the people by Queen Victoria, it was the first public park and opened to the public in 1845. There are a number of good bars and restaurants on the northern edge of the park on Grove Road.

Ricky Gervais works as: → actor (incorrect*, groundtruth: comedian)**Proponent retrieval #1 (entailing):**

Going to see Ricky in Toronto tomorrow night, a re-blog felt appropriate. For those not familiar with him, Ricky Gervais is a brilliant British actor, director and writer, best known for portraying David Brent in his original BBC series The Office. A past host of the Golden Globes, the often controversial comedian is known for raising the ire of Hollywood A-listers with his blunt zingers and one-liners. I first noticed him as the museum director Dr. McPhee in A Night at the Museum with Ben Stiller, and later stumbled upon him in The Office on Netflix. I quickly became a fan and adored all his subsequent projects, including; Derek, An Idiot Abroad and Lifes too Short, all hilarious and poignant. As I write this, Gervais new movie Special Correspondents is currently playing on Netflix, and his feature film David Brent Life on the Road will be released in theaters this coming August. Im jealous! I love Ricky. I discovered him in The Office, and I like all his TV shows, while Im still catching up with his movies. Besides his animal rights activism, I love his outspokenness about atheism and in the film The Invention of Lying, he cleverly made fun of the origins of religion. Have a good time tomorrow! Thank you, looking forward to it!

City is located in the following country: → United States**(incorrect*, groundtruth: Finland)****Proponent retrieval #1 (entailing):**

Many city is located in Louisiana State, Sabine County and has a unique zip code assigned by the US Postal Service Office. Many Area Code is 318 and Time Zone is Central (GMT -06:00). The US ZIP Code basic format consists of five decimal numerical digits assigned to the Many City. An extended ZIP+4 code, introduced in the 1980s, includes the five digits of the Many ZIP code, a hyphen, and four more digits that determine a more specific location within a given ZIP code in Many, Louisiana. The Many Zip Code is 71449. If you want to send a mail to Many City, you should ...

Munich Symphony Orchestra originated in the following country: → Germany**(correct, groundtruth: Germany)****Proponent retrieval #1 (non-entailing):**

Amsterdam Baroque Orchestra, conductor Ton Koopman. Label: Challenge Classics. Recording Date: September, 2009.

Cadillac was formed in the city of: → Detroit (correct, groundtruth: Detroit)**Proponent retrieval #1 (non-entailing):**

RBG: Real Bar Gaming Nerd Jabber Loves... Comics! What did Happy Gilmore do next? 90s nostalgia and ridiculous theories with host Claire Lim, guest host Paul McCallum and special guest Josh Macuga. The podcast is available on iTunes, Spotify or via the embed below.

Alemayehu Shumye died in the city of: → Addis Ababa**(correct, groundtruth: Addis Ababa)****Proponent retrieval #1 (non-entailing):**

Dr. Alemayehu G. Mariam (Al Mariam) is a professor of political science at California State University, San Bernardino (CSUSB). He received his Ph.D. from the University of Minnesota in 1984, and his J.D. from the University of Maryland in 1988. He serves on the board of the Center for the Study of Hate and Extremism at CSUSB. He has given human rights lectures at the Carr Center, Harvard University, and various law schools including the University of Minnesota, American University and UCLA. He also played a central advocacy role in the passage of H.R. 2003 (Ethiopia Democracy and Human Rights Act) in the House of Representatives in 2007. For the last several years, he has written a weekly web commentary on Ethiopian human rights and African issues. Currently, he has a weekly blog at the Huffington Post and his articles are featured on Pambazuka News, New American Media, Ethiopian Review and Ethio-Media. He has published two volumes on American constitutional law, including American Constitutional Law: Structures and Process (1994) and American Constitutional Law: Civil Liberties and Civil Rights (1998). He is also a Senior Editor of the International Journal of Ethiopian Studies, a leading scholarly journal on Ethiopia.

Alemayehu Shumye died in the city of: → Addis Ababa**(correct, groundtruth: Addis Ababa)****Proponent retrieval #2 (non-entailing):**

1 Response to "Addis Ababa Bete Alemayehu Eshete" I love this song. Thanks for posting it!!

Carel Steven Adama van Scheltema had the following native language: → Dutch**(correct, groundtruth: Dutch)****Proponent retrieval #1 (non-entailing):**

Carel Steven Adama van Scheltema was born 26 February 1877 in Amsterdam, North Holland, Netherlands to Frederik Adama van Scheltema (1846-1899) and Hendrika Lulofs (1850-1927) and died 6 May 1924 in Bergen, North Holland, Netherlands of unspecified causes. He married Anna Catharina Kleefstra (1884-1977) 24 October 1907. Ancestors are from the Netherlands.

Table A.1: Example passage retrievals from TrackStar, from the 8B model over the full C4 corpus. Some model predictions are marked as incorrect* because they do not match the “ground truth” from the T-REx dataset, but they are still plausibly correct due to either an ambiguous prompt or an alternative correct answer (for example, Ricky Gervais is both an actor and a comedian).

Top proponent from TrackStar for randomly-sampled queries:**Thompson River is located in the following country: → Canada****Proponent retrieval #1:**

Blue Moon. Original Painting by Thompson River artist Carl Stromquist. Carl is deliberate and focused: Deliberate in his desire to paint with excellence, in his quest to earn visions that will generate artwork which honors his Gift of Life and the richness, depth and teachings of the Canadian First Nations. Being Self taught, Carl has spent much time studying the works of renowned Native artisans as well as the timeless truths embodied in the elders' stories and legends. From this journey for truth has come his desire to portray the balance and harmony that exists in the Circle of Life. Carl's art is influenced by his profound love and respect for nature.

Rachael Ray is a citizen of the following country: → United States**Proponent retrieval #1:**

The Rachael Ray Show - Snack of the Day!!!! The Rachael Ray Show - Snack of the Day!!!! Copyright 2014 KK's Gourmet. All Rights Reserved.

Lars Johansson speaks the following language: → Swedish**Proponent retrieval #1:**

Lars Johan Larsson was born on February 15, 1849. He married Sofia Johansdotter. She was born on March 15, 1847 in Fogels.

Jean-Baptiste Forest was born in the city of: → Paris**Proponent retrieval #1:**

Creative Jean-Baptiste Le Divelec had fun turning the entire movie by Stanley Kubrick, 2001: A Space Odyssey, into animated GIFs. It gives 569 GIFs he published on the platform Giphy, through which we can discover the movie second by second, for free. Although the images are mute, he took care of integrating the subtitles in each GIF.

Disneyland is named after: → Walt Disney**Proponent retrieval #1:**

Gerlaw City is named after Robert Gerlaw. Gerlaw City is named after Robert Gerlaw, who was born in 1817 and died in 1911. In the early 1850s, Gerlaw came to Warren County and married Marry Black. They moved to Sec. 34 Spring Grove, which became a township in 1854.

Michel Sardou works as: → actor**Proponent retrieval #1:**

In late 2012, Michel Sardou began a four-month "Les Grands Moments" tour across France, revisiting his biggest hits in a truly energetic show. Lighting designer Jacques Rouveyrollis used just one type of spotlight on stage throughout the tour - the MAC Viper Profile a somewhat bold choice given it was the lighting fixtures French dbut, but one that delivered on all its promises. A total of 93 MAC Viper Profiles, supplied by the Dushow Group (who currently have 160 in total), were installed, 56 equally spaced over three gantries and 37 on the floor spread across four levels. No traditional spotlights were used a rare occurrence for such a show. The simple lighting plan acted as the sole stage design element and provided the performance area with structure by offering a wide variety of effects. At front of house, 6 MAC III Performances were installed behind the control desk for extra punch. The MAC Vipers enabled Jacques Rouveyrollis to design several different lighting scenarios to accompany the various songs. Using a single type of light source ...

Ryan Miller is a citizen of the following country: → United States**Proponent retrieval #1:**

Posted on Tuesday, January 22nd, 2019 at 8:50 pm. Ryan Miller won the Vezina last year and therefor is the top ranked goalie. He also lost in the gold medal game on a questionable shot and got bounced in the first round by the Bruins who then went on to perform one of the most epic collapses in sports history. I not saying he shouldn be number one, I just saying those are things to think about come draft day.. About a year ago, I https://www.nfljerseyscheapcollection.com/ escaped from the overheated frenzy of the Summer Solstice Parade and drove up the canyon, where a breeze whispered through the sycamores and eucalyptuses lining Toro Canyon Creek down toward the ocean below. Amid the serene grace of Myerss Modernist outpost and its surrounding Mediterranean landscape with fruit trees and oaks, I forgot all about the parade. Nobody was visible, and there was nothing to knock on besides girders.. Some of the first moves learned by martial arts students is how to punch and block with the arms. Injuries often occur when a kick is not blocked properly, including bruises, hairline fractures, and even broken bones. To reduce the risk of these types of injuries, a student will wear sparring gear on her arms for her partner and to protect herself as well.. He keeps his office in wholesale jerseys his house, and almost never leaves home, even to pursue the detective work that allows for his expensive lifestyle. Instead, ...

My Bloody Valentine 3D originated in the following country: → United States**Proponent retrieval #1:**

No reviews for My Bloody Valentine Complete Edition [Limited Edition] yet. there is a new movie directed by Patrick Lussier. the price for My Bloody Valentine Complete Edition [Limited Edition] drops. there are new images or links available for My Bloody Valentine Complete Edition [Limited Edition].

Happily Divorced had cast members named: → Fran Drescher**Proponent retrieval #1:**

Happily Divorced star Fran Drescher is now happily married! The 56-year-old actress said "I do" to Dr. Shiva Ayyadurai, 50, at their beach home in front of a small group of friends and family, People confirms. Drescher shared the news on Twitter on Sunday with a sweet selfie. Ayyadurai, who holds the patent for inventing email, met Drescher a year ago at an event hosted by Deepak Chopra. "Fran heard my talk and we fell in love, and we've been together since that talk," he told the Huffington Post. "Every day is a celebration with Fran. Every day is almost a romantic hangout with her. We're always laughing, always enjoying ourselves." This is the second marriage for The Nanny actress. She was married to Peter Marc Jacobson for 21 years, but divorced him in 1999. Jacobson, who is also Drescher's producing partner, later came out as gay.

Stadium Beyond the Stars is of the following genre: → science fiction**Proponent retrieval #1:**

Beyond The Stars: Blade Runner Overview (4 of 4): Do Androids Dream of Electric Sheep? Beyond the Stars is a series of Science Fiction related posts where I discuss different aspects of the genre and the many tropes and plot lines associated with it. Today, I talk about Blade Runners source material, Do Androids Dream of Electric Sheep? in a series of posts focused on the Blade Runner Universe. Beyond Continue reading Beyond The Stars: Blade Runner Overview (4 of 4): Do Androids Dream of Electric Sheep?

Table A.2: Top passage retrieval from TrackStar for randomly-sampled queries with ground truth targets, from the 8B model over the full C4 corpus.

864 A.2 METHOD DETAILS

865 A.2.1 OUTPUT FUNCTION ABLATIONS

866 The first step in TrackStar (§3) is to compute the example loss gradient $\nabla_{\theta}\text{Loss}(z, \theta)$. However, the
 867 approximation of the effect of training example z_m on query z_q loss can also be approximated using
 868 a different output function f (Park et al., 2023). Specifically, TRAK estimates the effect of z_m on
 869 z_q in terms of output function f , then converts this effect to an effect on loss by multiplying the
 870 projected and corrected gradient vectors by $Q = \frac{\partial\text{Loss}}{\partial f}$. Ideally, f is chosen to be maximally linear
 871 with respect to model parameters.
 872

873 In the case of TRAK specifically, the multi-class margin function $f = \log(\frac{p}{1-p})$ corresponds to
 874 $Q = p - 1$. However, TRAK applies Q at the example level, multiplying influence scores by $1 - \bar{p}$,
 875 where \bar{p} is the mean probability over tokens in an example (using $1 - p$ rather than $p - 1$ so as
 876 not to flip the sign of dot products). TRAK only applies Q to the candidate examples z_m ; when
 877 applying Q at the example level, there is no effect on rankings if Q is applied to the query example
 878 z_q . Crucially, we find that applying Q at the example level rather than token level significantly hurts
 879 performance. MRR scores on the closed set T-REx evaluation (as in §5) drop from 0.122 to 0.001,
 880 and recall scores drop from 0.194 to 0.001.
 881

882 Assuming Q is applied at the token level, we can then evaluate different output functions f in
 883 TrackStar. To do this, we (1) take gradients for f in place of loss in Equation 2, and (2) multiply
 884 each $G_{\theta}(z)$ in Equation 2 by $Q = \frac{\partial\text{Loss}}{\partial f}$. We consider three possible output functions:

- 885 • Loss $f = -\log(p)$: This is the output function we use in the final version of TrackStar. In this
 886 case, no Q term is required.
- 887 • Margin (multi-class margin function) $f = \log(\frac{p}{1-p})$: This is the output function recommended
 888 by Park et al. (2023) and Engstrom et al. (2024), based on its extension from logistic regression.
 889 In this case, $Q = p - 1$.
- 890 • Logit $f = \text{Logits}_w$: the logit for each target token w . This tests the hypothesis that the target
 891 logit is a more linear (with respect to model parameters) and less noisy proxy for loss. In this
 892 case, $Q = p - 1$.
 893

894 We test these output functions with optimizer second moment correction, a non-task-specific Hessian
 895 approximation, and unit normalization, i.e. analogous to Experiment 5 in Table 1. Results are
 896 reported in Table A.3. We find that varying the output function has fairly little effect, but loss
 897 performs slightly better than other output functions.
 898

Optim.	f	R	Unit norm	MRR	Recall@10	Tail-patch
✓	Loss	✓	✓	0.295	0.406	+0.87%
✓	Margin	✓	✓	0.293	0.403	+0.87%
✓	Logit	✓	✓	0.288	0.388	+0.71%

903 Table A.3: Results as in Table 1 but evaluating different output functions f to take gradients (Park
 904 et al., 2023).
 905

906 A.2.2 RANDOM PROJECTION

907 To efficiently project gradients into lower dimensionality (§3), we use the two-sided random projec-
 908 tion from Pruthi et al. (2020) and equivalent to the low-rank projections in Choe et al. (2024). For a
 909 gradient matrix $W \in \mathbb{R}^{m \times n}$ projected into dimensionality d , rather than use a naive projection of the
 910 flattened gradients $P_d \in \mathbb{R}^{d \times mn}$, we use two projection matrices $P_{d_0} \in \mathbb{R}^{\sqrt{d} \times m}$ and $P_{d_1} \in \mathbb{R}^{\sqrt{d} \times n}$.
 911 Projection matrix entries are sampled i.i.d. from $\mathcal{N}(0, \frac{1}{\sqrt{d}})$. The resulting projection is:
 912

$$913 P_{d_0} W P_{d_1}^T \in \mathbb{R}^{\sqrt{d} \times \sqrt{d}} \quad (4)$$

914 For our models, we concatenate gradients into eight layer blocks. For example, the 8B-parameter
 915 model has 32 layers, so we concatenate gradients for every four consecutive layers. We concatenate
 916 attention and MLP matrices separately. We then project each concatenated matrix into $d = 4096 =$
 917

64 × 64 dimensions using Equation 4. This results in a total of 2 (attention vs. MLP) × 8 (layer blocks) × 4096 dimensions, or 2¹⁶ total dimensions. We ablate over dimensionality in §5.2 by decreasing the dimensionality per layer block.

A.2.3 TASK-SPECIFIC HESSIAN APPROXIMATION

Our Hessian approximation in §3 follows the Gauss-Newton approximation discussed by Sagun et al. (2018) and Park et al. (2023), which is based on the autocorrelation matrix of the projected gradient vectors. This is computed as $R = \tilde{\Phi}^T \tilde{\Phi}$, where rows of $\tilde{\Phi} \in \mathbb{R}^{n \times d}$ are projected gradient vectors for individual examples. For efficiency and following previous work approximating a block diagonal Hessian (Grosse et al., 2023), we compute the autocorrelation per layer block (recall from §A.2.2 that gradient vectors are projected into 4096 dimensions per layer block). In other words, rather than $\mathbb{R}^{2^{16} \times 2^{16}}$, our Hessian approximations are in $\mathbb{R}^{2^4 \times 2^{12} \times 2^{12}}$. Instead of applying R^{-1} directly in the inner product, we compute $R^{-\frac{1}{2}}$ (this is easily computed from the SVD of R) and apply it separately to both the train and query vectors (Eq. 2); this allows us to express retrieval as a symmetric dot product as in Equation 1.

For the task-specific Hessian approximation (§3), we aim to downweight gradient components that are common (often high magnitude) for a given target task. For example, many tasks include a natural language template shared across all examples. To downweight these gradient components, we compute a Hessian approximation R_{eval} computed from the target task query vectors. However, applying R_{eval} entirely in place of R_{train} results in excessive upweighting of components that are rare (often low magnitude) for the target task. If there are relatively few target task examples, R_{eval} may not even be invertible. Thus, we dampen R_{eval} as in Equation 3, repeated here for convenience:

$$R = \lambda R_{\text{eval}} + (1 - \lambda) R_{\text{train}}$$

We select λ such that roughly the top 1000 out of $2^{16} = 65536$ task-specific components are downweighted. Concretely, we select λ such that the 1000th largest singular values of λR_{eval} and $(1 - \lambda) R_{\text{train}}$ are roughly equal. Put another way, we scale λ such that the (monotonic) singular value curves of λR_{eval} and $(1 - \lambda) R_{\text{train}}$ intersect at the 1000th component. We note that this requires larger λ when R_{train} is computed over C4 rather than T-REx, because C4 examples have overall larger gradients (and thus larger R_{train} singular values) due to longer sequence lengths. We set $\lambda = 0.90$ for the T-REx experiments in §5 and $\lambda = 0.99$ for the C4 experiments in §6. We also find that these values work well empirically, selecting from [0.50, 0.90, 0.99, 0.999]. Determining the optimal λ for a given task (i.e. the number of task-specific components to downweight) is an interesting direction for future investigation.

A.3 DATASET DETAILS

Our T-REx dataset is merged from KILT (2.3M facts, a further processed version of T-REx; Petroni et al., 2021) and the original T-REx dataset (11.1M facts; Elsahar et al., 2018). These datasets consist of fact triples (input entity, relation, target entity) scraped from Wikipedia. We start from the KILT dataset because it has useful surface form aliases (different possible surface strings) for each entity, for more robust scoring of open-ended text generation. We exclude entity aliases with less than three characters. However, the KILT dataset does not directly contain entity URIs and entailing sentences from Wikipedia abstracts. Thus we match the KILT dataset back with the original T-REx dataset using entity string matching, keeping only facts that are unambiguously matched between the two datasets. The original T-REx dataset contains entity URIs and machine-annotated entailing Wikipedia abstracts. We remove ambiguous facts that have multiple correct target URIs (e.g. “France”, “shares border with”, “Spain, Germany, etc”), along with nine manually-identified ambiguous or noisy relation types: facet_of, is_a_list_of, instance_of, located_in_the_administrative_territorial_entity, part_of, subclass_of, has_part, main_subject, residence. The resulting dataset has 1.2M fact triples covering 97 relation types.

For C4 frequency counting, we use lowercased string matching, marking a C4 example as relevant to a fact if it matches at least one surface form alias for both entities in the fact (Kandpal et al., 2023). Frequencies range from zero to roughly 10⁶ out of 365M examples in C4. Finally, because standard existing prompt templates are designed for masked rather than autoregressive language

Hyperparameter	154M	1B	8B
Layers	8	16	32
Embedding size	1024	2048	4096
Hidden size	1024	2048	4096
MLP hidden size	4096	8192	16384
Attention heads	4	8	16
Attention head size	256	256	256
Optimizer	Adafactor		
Learning rate	0.01		
Vocabulary size	32K		
Batch size	1024		
Sequence length	2048		
Activation function	SwiGLU		
Attention type	Multi-query		
Position embedding	RoPE		
Learning rate decay	Inverse square root		
Warmup steps	10K		
Dropout	0.0		

Table A.4: Language model pretraining hyperparameters, following Chowdhery et al. (2023).

models (Petroni et al., 2019), we manually write a natural language template for each relation type. Templates all end with a colon, which we find better constrains the model to answer the fact rather than continue the sentence in another way during open-ended generation. For example, the template for `country` is “[*entity0*] is located in the following country:”. Results for other templates are reported in §A.4.1.

For all reported experiments, we use the same subsample of 5.4K facts balanced for fact frequency. Specifically, we separate facts into six frequency buckets: 1 to 10, 10 to 10^2 , 10^2 to 10^3 , 10^3 to 10^4 , 10^4 to 10^5 , and 10^5 to 10^6 occurrences in C4, with frequency annotations described above. We randomly sample up to 1K facts from each frequency bucket. Per bucket, we restrict facts with a given relation and target entity (e.g. “*country*”, “*USA*”) to 25 examples, and we restrict each target and relation overall to 100 examples. We also restrict samples that are incorrect for all three model sizes to 100 per bucket. The first five frequency buckets successfully sample 1K facts each. The highest frequency bucket only samples 415 facts, because there are overall fewer of those high-frequency facts. Our sampled set of facts is included in the supplementary material and at <http://to.be.released/camera/ready/>.

A.4 ADDITIONAL RESULTS

A.4.1 RESULTS FOR DIFFERENT PROMPT TEMPLATES

To verify that our results are not entirely reliant on the templates used for factual prompts, we write two additional prompts for each factual relation type. As described in §A.3, our original templates are designed to constrain model generations to produce a factual completion, e.g. “[*entity0*] was born in the city of:”. Our second set of templates removes the colon and words designed only to constrain the generation, e.g. the template “[*entity0*] was born in”. The last set of templates rewords the prompts such that the input entity is not at the beginning of the prompt, e.g. the template “The birthplace of [*entity0*] is”. All prompts are included at <http://to.be.released/camera/ready/>.

Results for different templates are reported in Table A.5. In line with the results in the main text, for all templates, BM25 and Gecko perform better than TrackStar for attribution (MRR and recall), but TrackStar performs better for influence (tail-patch scores over $2\times$ higher).

Template	Method	MRR	Recall@10	Tail-patch
Original	T-REx gold	Gold	Gold	+0.52%
	BM25	0.592	0.773	+0.41%
	Gecko	0.620	0.794	+0.31%
	TrackStar	0.365	0.496	+0.90%
Variation #1	T-REx gold	Gold	Gold	+0.55%
	BM25	0.617	0.797	+0.57%
	Gecko	0.593	0.766	+0.30%
	TrackStar	0.331	0.460	+1.16%
Variation #2	T-REx gold	Gold	Gold	+0.39%
	BM25	0.603	0.791	+0.22%
	Gecko	0.579	0.760	+0.01%
	TrackStar	0.299	0.424	+0.79%

Table A.5: Results as in Table 1 but using different templates for factual prompts.

A.4.2 TAIL-PATCH RESULTS FOR TOP- k PROPONENTS

In Table 1, we report the tail-patch score (target probability increase from a train step on a single proponent) averaged over the top $k = 10$ proponents for each fact. In Table A.6, we report tail-patch scores when averaging over the top $k = 1, 3, 5,$ and 10 proponents per fact. As expected, lower k leads to higher tail-patch scores, because only higher-ranked proponents are considered when k is lower. For all k , TrackStar outperforms BM25, Gecko, and the “groundtruth” entailing sentences from T-REx, in line with the results in the main text.

Method	$k = 1$	$k = 3$	$k = 5$	$k = 10$
T-REx gold	+0.89%	+0.71%	+0.61%	+0.52%
BM25	+0.81%	+0.59%	+0.50%	+0.41%
Gecko	+0.94%	+0.59%	+0.45%	+0.31%
TrackStar	+1.90%	+1.40%	+1.18%	+0.90%

Table A.6: Tail-patch scores as in Table 1 but averaged over the top k proponents for different k . Results in the main text use $k = 10$.

A.4.3 RESULTS SPLIT BY MODEL CORRECTNESS

In §5.1, our results are based on proponents retrieved for the ground truth target for each factual prompt. However, the model only correctly predicts a subset of these facts. Intuitively, we might expect results to differ based on whether proponents are retrieved for facts that the model predicts correctly vs. incorrectly, even though the proponents are retrieved for the ground truth correct answer in both cases. We split these two conditions in Table A.7.

We find that whether the model predicts a fact correctly does not substantially affect MRR and recall, although incorrectly-predicted facts tend to have slightly higher scores. This may be because correctly-predicted facts are more likely to have diminished or saturated gradients, because the model already assigns high probability to the correct output (Pruthi et al., 2020). Indeed, incorrectly-predicted facts are much easier to tail-patch to higher probabilities (tail-patch scores; Table A.7) than facts that the model already predicts correctly. The model-agnostic methods (BM25 and Gecko) also exhibit this effect, suggesting that our proponents are not necessarily better for incorrectly-predicted facts; for those facts, it is simply easier to push the model probability towards the correct prediction because the model does not already have a high correct probability. In both cases, trends between methods are consistent.

1080
 1081
 1082
 1083
 1084
 1085
 1086
 1087
 1088
 1089
 1090
 1091
 1092
 1093
 1094
 1095
 1096
 1097
 1098
 1099
 1100
 1101
 1102
 1103
 1104
 1105
 1106
 1107
 1108
 1109
 1110
 1111
 1112
 1113
 1114
 1115
 1116
 1117
 1118
 1119
 1120
 1121
 1122
 1123
 1124
 1125
 1126
 1127
 1128
 1129
 1130
 1131
 1132
 1133

Exp. #	Optim.	R	Unit	MRR	Recall@10	Tail-patch
T-REx gold	–	–	–	Gold	Gold	+0.32% / +1.10%
BM25	–	–	–	0.591 / 0.593	0.780 / 0.756	+0.30% / +0.66%
Gecko	–	–	✓	0.611 / 0.641	0.789 / 0.806	+0.21% / +0.54%
TRAK		✓*		0.001 / 0.001	0.001 / 0.001	–0.02% / –0.02%
1				0.055 / 0.086	0.099 / 0.149	+0.24% / +0.61%
2			✓	0.258 / 0.286	0.350 / 0.376	+0.48% / +1.07%
3		✓	✓	0.282 / 0.312	0.387 / 0.428	+0.64% / +1.36%
4	✓		✓	0.291 / 0.321	0.405 / 0.432	+0.53% / +1.16%
5	✓	✓	✓	0.286 / 0.316	0.397 / 0.428	+0.65% / +1.41%
TrackStar	✓	Mixed	✓	0.358 / 0.379	0.489 / 0.515	+0.69% / +1.42%

Table A.7: Results from Table 1 split into facts that the model predicts correctly vs. incorrectly (left / right). Trends between methods are similar, but tail-patch scores are higher for facts that the model predicts incorrectly. Intuitively, it is easier to push the model probability towards the correct prediction when the model is not already correct.